

STRENGTH CHARACTERISTICS OF RESORBABLE OSTEOCONDUCTIVE CERAMICS BASED ON DIPHOSPHATES OF CALCIUM AND ALKALI METALS

V. I. Putlayev,¹ P. V. Evdokimov,¹
A. V. Garshev,¹ D. V. Prosvirin,² E. S. Klimashina,¹
T. V. Safronova,¹ and V. K. Ivanov³

UDC 546.41:546.185:617:666.3:666.1:666.9

An investigation into the strength characteristics of ceramics based on diphosphates $\text{Ca}_{(3-x)}\text{M}_{2x}(\text{PO}_4)_2$ ($x = 0-1$ and $\text{M} = \text{Na}, \text{K}$) provides evidence of composition strengthening in the range $x = 0.6-0.8$ containing the greatest amount of the supercooled high-temperature modification $\alpha\text{-CaMPO}_4$. The method of high-temperature x-ray diffractometry is used to examine thermal expansion of rhenanite phases of CaMPO_4 .

Keywords: strength, fracture toughness, thermal expansion, ceramics, calcium phosphates, phase transition, twinning.

INTRODUCTION

Synthetic biomaterials are widely used as implants for reconstruction of injured human tissues. Their biocompatibility (both chemical and physical) is a primary object of study at the present time. The fabrication of materials with the intrinsic properties of parts of the human body is a major thrust in the synthesis of biomaterials [1].

Bone is a biocomposite with multilevel organization. It fulfills a multiplicity of functions, including that of support [2]. Despite its high density ($\sim 2 \text{ g/cm}^3$), bone possesses distinctive mechanical characteristics (high strength and significant resistance to fracture).

Calcium phosphates are one of the most important biomaterials for replacement of bone tissue. At present, biomaterials based on hydroxyapatite (HA, $\text{Ca}_{10}(\text{PO}_4)_6(\text{OH})_2$) are widely used, along with biomaterials based on more soluble tricalcium phosphate (TCP, $\text{Ca}_3(\text{PO}_4)_2$) [3, 4]; however, even TCP does not satisfy all of the requirements that biomaterials should possess (biosolubility, strength, fracture toughness, etc.). It is proposed to use diphosphates of calcium and alkali metals with the general formula $\text{Ca}_{(3-x)}\text{M}_{2x}(\text{PO}_4)_2$ ($x = 0-1$, $\text{M} = \text{Na}, \text{K}$) and the structure of β -TCP (for $x < 0.15$) and the glaserite-like phases of CaMPO_4 (rhenanite for $x = 1$) as components of ceramics or multiphase composites intended to replace bone tissues, possessing an enhanced level of solubility and superior mechanical characteristics in comparison with HA and TCP.

The phase relationships in the indicated systems are characterized by a quite complex polymorphism and the presence of intermediate compounds (Fig. 1) [5]. Synthesis of ceramic composites in the given systems presupposes knowledge of the dependence of the strength characteristics on composition. Moreover, anisotropic thermal expansion of low-symmetry glaserite phases is capable of inducing cracking of the ceramic. At the same time, studies of thermal expansion of rhenanites (CaMPO_4) are lacking at the present time. The above-enumerated aspects of bioceramics based on diphosphates were thus chosen as the subject of the present work.

¹M. V. Lomonosov Moscow State University, Moscow, Russia; ²A. A. Baikov Institute of Metallurgy and Materials Science of the Russian Academy of Sciences, Moscow, Russia; ³N. S. Kurnakov Institute of General and Inorganic Chemistry, Moscow, Russia, e-mail: valery.putlayev@gmail.com. Translated from *Izvestiya Vysshikh Uchebnykh Zavedenii, Fizika*, No. 10, pp. 72–77, October, 2013. Original article submitted August 6, 2013.

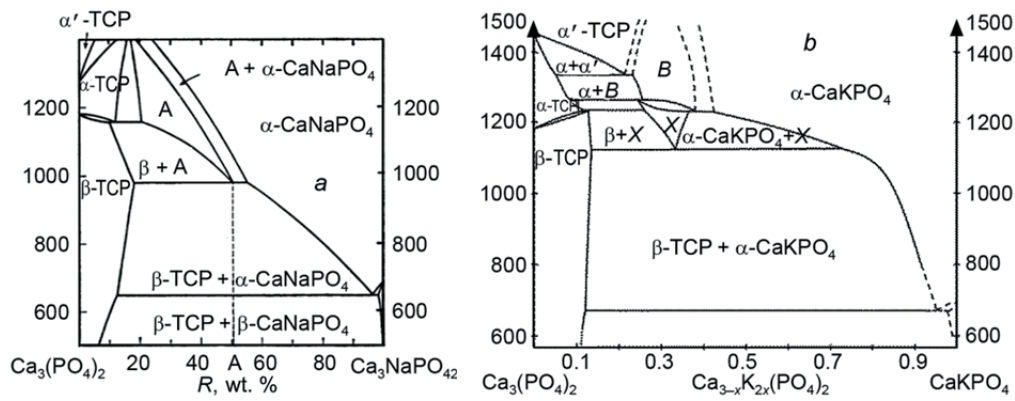


Fig. 1. Phase diagrams of $\text{Ca}_3(\text{PO}_4)_2 - \text{CaNaPO}_4$ (a) and $\text{Ca}_3(\text{PO}_4)_2 - \text{CaKPO}_4$ (b).

OBJECTS AND METHODS OF STUDY

To synthesize diphosphates of calcium and alkali metals, we chose the following scheme:



where $M = \text{Na}, \text{K}$ and $x = 0-1$. The reaction mixture was ground in a Pulverisette (Fritsch, Germany) planetary ball mill in an acetone medium. The milled mixture was passed through a Saatilene HiTech™ polyester sieve with pore size $\sim 200 \mu\text{m}$ and then poured into an alundum crucible and fired in the temperature interval $800-1100^\circ\text{C}$ for up to 12 h. A plasticizer (paraffin, 10% by mass of the powder) was added to disaggregated powders after firing. From the pressed powder we formed small bars on a Carver C (USA) manual lab press at a pressure of $\sim 2 \text{MPa}$. The thus-obtained small bars were sintered at a temperature of 1200°C .

X-ray diffraction (XRD) measurements were performed at temperatures from 50 to 1250°C *in situ* using an HT-1500 high-temperature attachment on a Rigaku D/MAX 2500 diffractometer with a rotating anode (Rigaku, Japan). The analysis was performed in a platinum sample holder. The diffraction patterns were recorded in reflection mode (Bragg-Brentano geometry) using $\text{CuK}_{\alpha\text{v}}$ radiation (wavelength $l = 1.54183 \text{ \AA}$). The working parameters of the generator were: accelerating voltage 40 kV and tube current 200 mA . The patterns were recorded in the platinum sample holder. Profile analysis of the spectra and determination of values of the lattice parameters were carried out using the *WinXPOW* software package (STOE GmbH).

The sample compression tests at room temperature were performed according to GOST 8462-85 and GOST 25.503-97 standard specifications with a testing rate of 1 mm/min from a calculation of 5 samples per point. The single column testing system Instron 5848 MicroTester (Instron, UK) met GOST 28840 specifications. The distance between the supports was 10 mm . The bending strength for each sample was calculated according to the formula

$$\sigma = (3Wl) / (2bd^2), \quad (2)$$

where σ is the limit of bending strength, MPa, W is the destructive load, N, l is the distance between supports, mm, b is the width of the test sample (length of the side perpendicular to the direction of application of the load), mm, and d is the thickness of the sample (length of the side parallel to the direction of application of the load), mm.

We calculated the fracture toughness K_{IC} using the Evans-Charles formula [6]

$$K_{\text{IC}} = 0.0752PC^{-3/2}, \quad (3)$$

TABLE 1. Unit Cell Parameters of CaNaPO₄ vs. Temperature

Parameter	Unit Cell Parameters of CaNaPO ₄ vs. Temperature	
	$T < 680^{\circ}\text{C}$	$T > 680^{\circ}\text{C}$
$a, \text{\AA}$	$20.378(3) + 1.45(88) \cdot 10^{-4} \cdot T + 7.23 \cdot 10^{-7} \cdot T^2$	
$b, \text{\AA}$	$5.406(1) + 4.31(12) \cdot 10^{-5} \cdot T$	
$c, \text{\AA}$	$9.1545(47) + 2.25(9) \cdot 10^{-4} \cdot T$	
$a, \text{\AA}$		$5.324(2) + 9.774(184) \cdot 10^{-5} \cdot T$
$c, \text{\AA}$		$7.0772(5) + 3.817(56) \cdot 10^{-4} \cdot T$
$V, \text{\AA}^3$	$83.95(8) + 0.0053 \cdot T$	$173.16(6) + 0.1658(16) \cdot T$

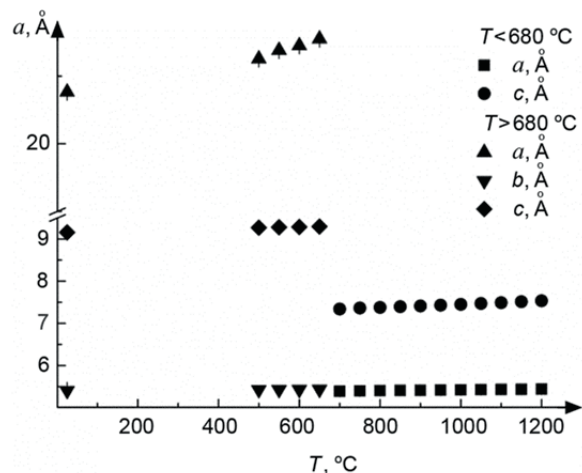


Fig. 2

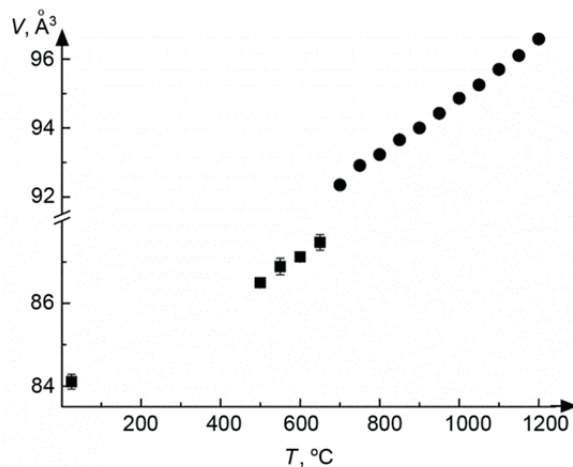


Fig. 3

Fig. 2. Variation of the lattice parameters of CaNaPO₄ as a function of temperature.

Fig. 3. Variation of the volume of the unit cell of CaNaPO₄ as a function of temperature.

where P is the applied load upon indentation and C is the length of a median crack. To measure the fracture toughness, we applied a 1-kg load (loading time 30 s) to the surface of ceramic samples with the help of a 402-MVD micro Vickers hardness tester (indenter) (Wolpert Group, UK)

The microstructure of the samples was investigated using a LEO SUPRA 50VP (Carl Zeiss, Germany) scanning electron microscope with field-emission source. For this purpose, a layer of carbon or gold was deposited on the samples using a QT-150T ES sputter coater (Quorum Technologies, UK). The accelerating voltage was 3–10 kV. Images were obtained with magnifications up to 100000^x with the help of an SE2 secondary electron detector (Carl Zeiss, Germany).

RESULTS AND DISCUSSION

Coefficient of Thermal Expansion of CaMPO₄

We first obtained dependences (Table 1) of the variation of the linear parameters (Fig. 2) and volume (Fig. 3) of the unit cell of CaNaPO₄ on the temperature. Toward this end, we used Al₂O₃ as an internal standard. According to the law of variation of the coefficient of thermal expansion ($\alpha = 2.081(57) \cdot 10^{-5} + 0.660(48) \cdot 10^{-8} T$ in one direction in the basal plane and along the c axis $\alpha = 2.137(286) \cdot 10^{-5} + 0.627(139) \cdot 10^{-8} T - 0.134(62)/T^{-2}$ [7]) we determined the

TABLE 2. Dependence of the Parameters of the Unit Cell of CaKPO₄ on Temperature

Parameter	Law of variation of the parameter as a function of temperature for the pure phase of CaKPO ₄
	$T > 680^{\circ}\text{C}$
$a, \text{Å}$	$5.454(7) + 1.96(17) \cdot 10^{-4} \cdot T - 4.75(91) \cdot 10^{-8} \cdot T^2$
$c, \text{Å}$	$7.65(1) - 1.42(12) \cdot 10^{-4} \cdot T + 1.73(6) \cdot 10^{-7} \cdot T^2$
$V, \text{Å}^3$	$197.78(22) + 8.55(9) \cdot 10^{-3} \cdot T + 2.29(34) \cdot 10^{-6} \cdot T^2$

interplanar distances, which should correspond to the locations of the diffraction peaks of Al₂O₃ in the x-ray diffraction pattern at the given temperature. Thus, the zero position of the goniometer was corrected for each temperature and taking this parameter into account we calculated the parameters of the unit cell of CaNaPO₄ as a function of temperature. In Fig. 3 it is possible to clearly distinguish a significant jump in the volume upon a change in the modification of CaNaPO₄ from the low-temperature phase to the high-temperature phase. The significant recorded change in volume ($\Delta V/V = +5.6\%$) can lead to negative consequences (accumulation of mechanical stresses in the sample, which can then lead to formation and development of cracks) in any attempt to obtain dense ceramic materials based on a pure phase of CaNaPO₄.

According to our data, the fast first-order phase transition α/β -CaNaPO₄ bears a deformational character and is associated with small (less than interatomic distances) cooperative displacements of atoms in the cation–anion columns of the glaserite structure and, in a fundamental way, with rotations of the phosphate tetrahedra. This is reminiscent of the situation with the α/α' -Ca₃(PO₄)₂ transition [8], and synthesis of a single-phase product containing only the high-temperature phase α -CaNaPO₄ is thus impossible. It makes sense to assume a similar structural pattern for α -Ca₃(PO₄)₂ and β -CaNaPO₄, the same as for α' -Ca₃(PO₄)₂ and α -CaNaPO₄, and it correspondingly also makes sense to assume the possibility of formation of a continuous series of solid solutions, at any rate, between the latter two phases at high temperatures.

From a comparison with the α/β -CaNaPO₄ phase transformation, the first-order phase transition α/β -CaKPO₄ is kinetically hindered, which is clearly connected with the large ionic radius of K in comparison to Na, leading to a slower displacement of cations in the columns and impeded rotation of phosphate tetrahedra. From the high-temperature XRD data, the β/α -CaKPO₄ transition takes place in the temperature region $(675 \pm 25)^{\circ}\text{C}$; however, supercooling can exceed 200°C . This makes it possible to obtain a single-phase product containing only the α -CaKPO₄ high-temperature phase via rapid cooling. In analogy with the study on CaNaPO₄ we calculated the laws of variation of the lattice parameters, and also of the volume of the unit cell, for CaKPO₄ (Table 2). Note that the β/α -CaKPO₄ transition is accompanied by a negative volume effect $\Delta V/V = -2\%$. Expansion upon cooling leads to cracking or even fracture of a dense CaKPO₄ based ceramics.

Strength Characteristics of CaMPO₄

Analysis of the density of the ceramics (Fig. 4) shows that the greatest increase in density is observed for compositions with $x = 0.5$ – 0.7 , while compositions with $x = 0.1$ – 0.4 sinter most poorly. We associate the poor sintering of compositions with low Na content a) with poorer diffusion mobility of Ca²⁺ in comparison with Na⁺ and b) with the conversion of $\alpha \rightarrow \beta$ -TCP upon cooling [9].

Our study of the strength characteristics of dense ceramics (Fig. 5) shows that the bending strength is higher for intermediate compositions Ca_(3-x)M_{2x}(PO₄)₂ $x = 0.6$ – 0.7 for Na and $x = 0.7$ for K. The extremal course of the dependence of the strength on composition correlates with the density of the ceramics although it cannot be explained completely by just a difference in density.

It should be noted that micro-cracking is observed in all the obtained samples as a consequence of anisotropy of the change in dimensions during the β/α transition in CaNaPO₄; nevertheless, this does not lead to spontaneous fracture of the ceramics, but the samples with $x = 0.6$ – 0.8 demonstrate bending strength that is not less than 10 MPa. The propagation of a crack in the ceramics is associated with peculiarities of their microstructure (Fig. 6). Different steps in

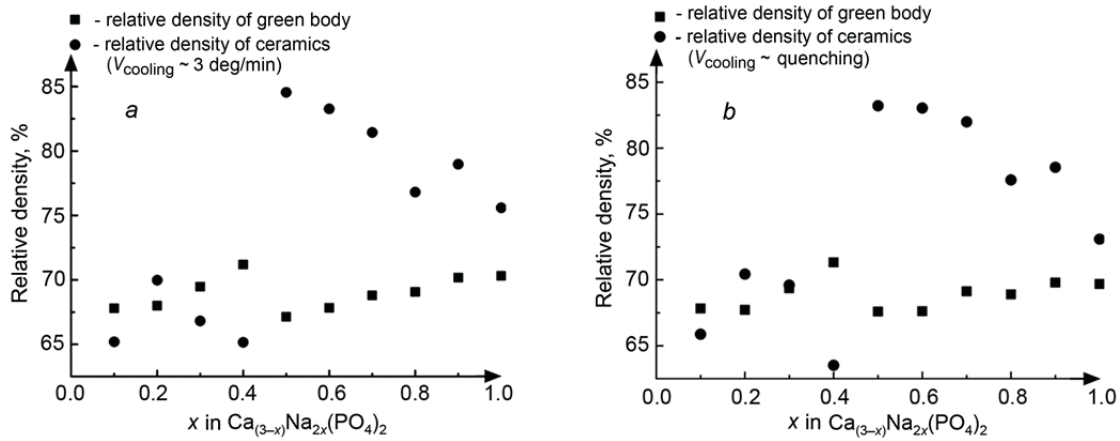


Fig. 4. Comparison of the dependence of the relative density of green body and ceramics $\text{Ca}_{(3-x)}\text{Na}_{2x}(\text{PO}_4)_2$ on composition (x): *a*) gradual cooling of the ceramic samples, cooling rate equal to 3 deg/min, and *b*) quenching of the ceramic samples.

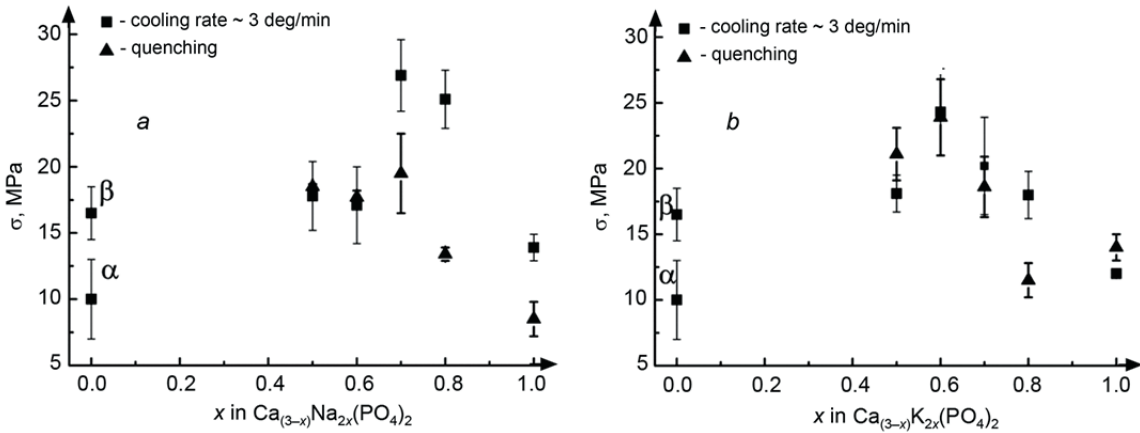


Fig. 5. Comparison of the dependence of the bending strength of ceramic samples obtained with different cooling rates on the composition (x): *a*) bending strength of the $\text{Ca}_{(3-x)}\text{Na}_{2x}(\text{PO}_4)_2$ based ceramics, and *b*) bending strength of the $\text{Ca}_{(3-x)}\text{K}_{2x}(\text{PO}_4)_2$ based ceramics.

the etching of polished ceramic surface (in the process of modeling their resorption in media with different pH) reveal merohedric twinning of grains.

The cause of twinning is the $\alpha \rightarrow \beta$ transition in NaCaPO_4 , which is associated with a lowering of the symmetry from $P\bar{3}m1$ to $P2_1/a$ in the glaserite structure. We carried out a group-theoretic analysis of the transition, which showed that lowering of the symmetry for an invariant type of the Bravais lattice is accompanied by a lowering of the order of the point symmetry group by three – from $\bar{3}m$ to $2/m$. This gives three different orientations of the twin boundaries (Fig. 6*b*). The thickness of the twin lamellae decreases with growth of x . Thus, the strengthening mechanism can be associated both with a decrease of the characteristic scale of an element of the microstructure and with a reorientation of the crack during the transition from one system of lamellae to another. The question of the potential possibility of applying an external mechanical stress to the supercooled high-temperature phase of rhenanite to induce twinning (i.e., in fact to provide for a dissipation channel for the elastic energy liberated upon the opening of a crack) remains open. However, the very fact of the relaxation of the elastic energy accumulated in a grain as a result of the transition, in the form of twinning, speaks of the possibility of such a dissipative channel.

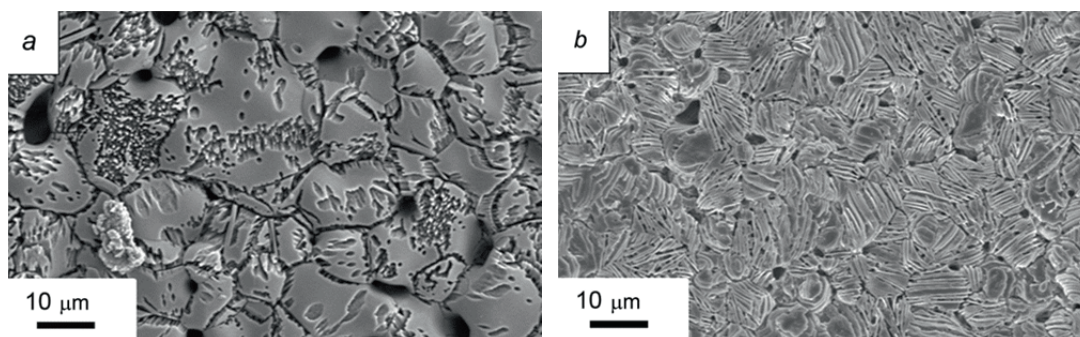


Fig. 6. Microstructure of samples of the ceramics $\text{Ca}_{(3-x)}\text{Na}_{2x}(\text{PO}_4)_2$, where $x = 0.4$, after runs of dissolving in tris-buffer with $\text{pH} = 7.4$ (a) and in water with $\text{pH} = 6.5$ (b).

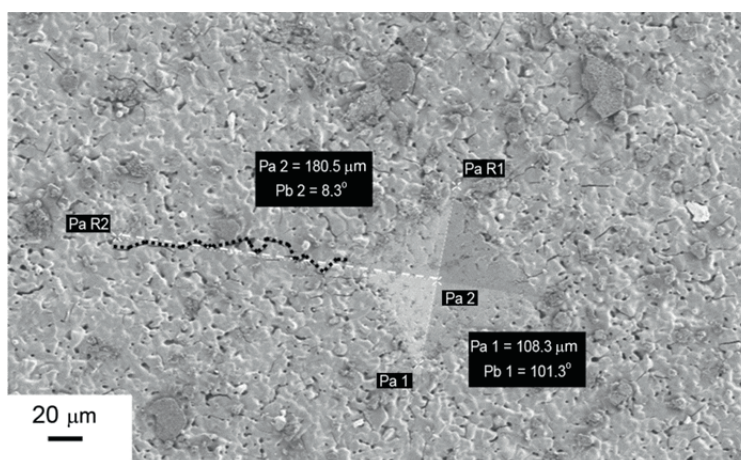


Fig. 7. Microphotograph of the surface of a ceramic sample with an indent of Vickers pyramid; the black dotted wandering line indicates the trajectory of a median crack.

Figure 7 displays a microphotograph of a Vickers indentation on the surface of a ceramic bar. It can be seen that the median crack bears both an intergranular and a transgranular character. The trajectory of its propagation allows one to conclude that the main mechanisms of braking of the crack are its reorientation and branching. Fracture toughness, estimated from the length of the median cracks around a Vickers indentation (Fig. 8), as in the case of bending strength, passes through a maximum, varying from 0.3 for extreme compositions to $0.9 \text{ MPa}\cdot\text{m}^{1/2}$ for intermediate compositions containing the greatest amount of the supercooled high-temperature modification $\alpha\text{-CaMPO}_4$.

CONCLUSIONS

Our investigation into the strength characteristics of ceramics based on diphosphates $\text{Ca}_{(3-x)}\text{M}_{2x}(\text{PO}_4)_2$ ($x = 0-1$, $\text{M} = \text{Na}, \text{K}$) provides evidence of strengthening of compositions in the range $x = 0.6-0.8$ containing the greatest amount of supercooled high-temperature modification $\alpha\text{-CaMPO}_4$. Propagation of cracks in similar composites is associated with peculiarities of the $\alpha/\beta\text{-CaMPO}_4$ phase transformations. The diffusionless transformation $\beta \rightarrow \alpha$ in pure rhenanite CaMPO_4 during heating is associated with rotations of the tetrahedra and is accompanied by a change in volume. It is obvious that the transformation rate can be controlled by increasing the Ca content in the high-temperature phase since in this case the excess amount of calcium should redistribute itself diffusively between $\beta\text{-CaMPO}_4$ and $\text{Ca}_3(\text{PO}_4)_2$. This

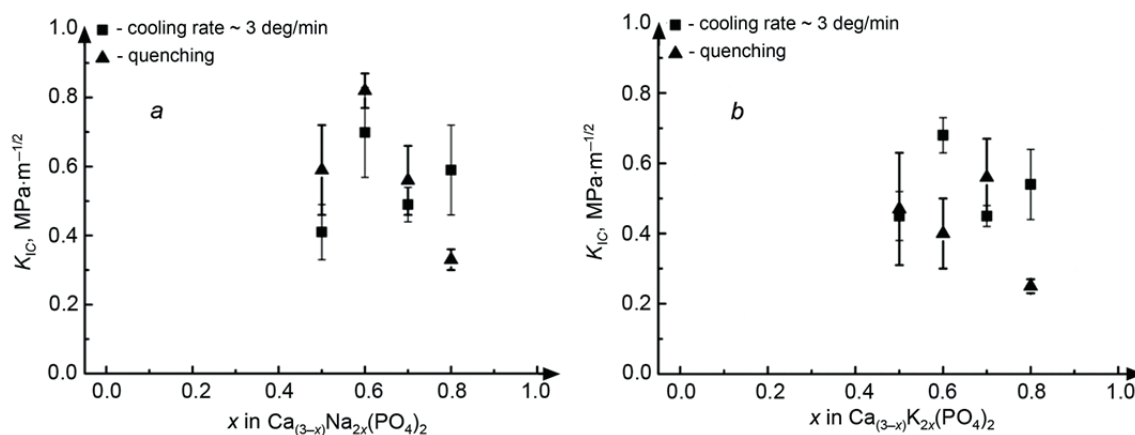


Fig. 8. Comparison of the dependence of fracture toughness of ceramic samples obtained at different cooling rates on the composition (x): *a*) fracture toughness of ceramic materials based on $Ca_{(3-x)}Na_{2x}(PO_4)_2$ and *b*) fracture toughness of ceramics based on $Ca_{(3-x)}K_{2x}(PO_4)_2$.

makes it possible to control the $\beta \leftrightarrow \alpha$ transformation of rhenanite as a function of composition and cooling rate; in this regard, the potential possibility exists of converting the supercooled α -phase of rhenanite into the low-temperature β -modification in the elastic stress field arising at the tip of the crack. The availability of this mechanism would mean the appearance of a new dissipation channel for the elastic energy liberated upon the opening of the crack and could lead to a lowering of the stress intensity factor and an increase in the volume of the pseudoplastic zone at the tip of the growing crack.

This work was performed using equipment acquired through the resources of the Program for Development of Moscow State University. This research was supported by grants from the Russian Foundation for Basic Research Nos. 12-03-01025, 12-08-00681, 12-08-33125 mol_a_ved, 13-08-12236 ofi_m, and 13-08-01056.

REFERENCES

1. L. L. Hench, *J. Am. Ceram. Soc.*, **81**, 1705–1727 (1998).
2. R. H. Doremus, *J. Mat. Sc.*, **27**, 285–297 (1992).
3. A. Ito and R. Le Geros, *Z. Key Eng. Mater.*, **377**, 85–98 (2008).
4. D. Tadic and M. Epple, *Biomater.*, **25**, 987–994 (2004).
5. P. V. Evdokimov, V. I. Putlayev, *et al.*, Proceedings of the Conference on the Investigation of Materials Using the Methods of Thermal Analysis, Calorimetry, and Gas Sorption [in Russian], Saint Petersburg (2012), pp. 123–128.
6. A. G. Evans and E. A. Charles, *J. Am. Ceram. Soc.*, **59**, 371–372 (1976).
7. G. Fiquet, P. Richet, and G. Montagna, *Phys. Chem. Min.*, **27**, 103–111 (1999).
8. M. Yashima, and A. Sakai, *Chem. Phys. Lett.*, **372**, 779–783 (2003).
9. P. V. Evdokimov, V. I. Putlayev, D. A. Merzlov, *et al.*, *Nanosistemy: Fizika, Khimiya, Matematika*, **4**, No. 2, 48–54 (2013).